Heliyon 10 (2024) e37900

Contents lists available at ScienceDirect

Heliyon

journal homepage: www.cell.com/heliyon

Research article

HIF-1α knockdown suppresses breast cancer metastasis via epithelial mesenchymal transition Abrogation

Jinjin Zhao [a,d], Haiguang Zhang [b], Yaqian Liu [c,d], Guangjian Lu [a], Zhaohui Wang [a], Qingjiang Mo [a], Guoqiang Wang [a], Yanfei Shen [a,e,**], Luyang Jiao [a,f,*]

[a] Clinical Laboratory, The First Affiliated Hospital of Xinxiang Medical University, Xinxiang, Henan, 453100, China
[b] Department of Gynecology, The First Affiliated Hospital of Xinxiang Medical University, Xinxiang, Henan, 453100, China
[c] Otorhinolaryngology, The First Affiliated Hospital of Xinxiang Medical University, Xinxiang, Henan, 453100, China
[d] Life Science Research Center, The First Affiliated Hospital of Xinxiang Medical University, Xinxiang, Henan, 453100, China
[e] Medical School, Southeast University, Nanjing, Jiangsu, 210009, China
[f] Department of Blood Transfusion, The First Affiliated Hospital of Xinxiang Medical University, Xinxiang, Henan, 453100, China

ARTICLE INFO

Keywords:
HIF-1α
EMT
Breast cancer
Lung metastasis
Mice

ABSTRACT

Lung metastasis, a leading cause of breast cancer mortality, lacks effective therapeutic options. Hypoxia-inducible factor 1-alpha (HIF-1α) plays important roles in breast cancer progression, but its direct impact on lung metastasis remains unclear. Herein, in this study, we investigated the role of HIF-1α in breast cancer lung metastasis and the potential of targeting it for therapeutic benefit. HIF-1α expression was knocked down in the 4T1 mouse mammary carcinoma cell line using a lentiviral vector. HIF-1α knockdown significantly reduced the migratory ability of 4T1 cells in vitro and lung metastasis in a mouse model. Mechanistically, HIF-1α knockdown decreased the expression of matrix metalloproteinases (MMP-2 and MMP-9) that degrade the extracellular matrix and suppressed the epithelial-to-mesenchymal transition (EMT) by increasing E-cadherin and decreasing vimentin expression. The findings of this study demonstrate that HIF-1α knockdown effectively inhibits lung metastasis of 4T1 cells both in vitro and in vivo by suppressing EMT. These results underscore a promising new approach for managing breast cancer metastasis.

1. Introduction

Breast cancer is the most prevalent malignancy worldwide; however, with the continuous improvement in treatment methods, the survival times of patients have improved notably [1,2]. However, patients with metastatic breast cancer still face poor survival rates [3], and more than 90 % of breast cancer patients succumb to this disease due to metastasis [4]. Exploring the mechanism of distant metastasis will help develop effective treatment for the management of breast cancer [5].

Epithelial Mesenchymal Transition (EMT) and angiogenesis are well-established factors that contribute to tumor metastasis [6]. During EMT, epithelial cells lose their characteristic properties and gain mesenchymal traits, which enables cancer cells to migrate and invade surrounding tissues, ultimately promoting metastasis from the primary tumors [7–9]. It is well known that EMT and hypoxia

* Corresponding author. Clinical Laboratory, The First Affiliated Hospital of Xinxiang Medical University, Xinxiang, 453100, China.
** Corresponding author. Clinical Laboratory, The First Affiliated Hospital of Xinxiang Medical University, Xinxiang, Henan, 453100, China.
E-mail addresses: yanfei.shen@seu.edu.cn (Y. Shen), jiaoluyang2009@163.com (L. Jiao).

https://doi.org/10.1016/j.heliyon.2024.e37900
Received 24 June 2024; Received in revised form 12 September 2024; Accepted 12 September 2024
Available online 14 September 2024

can activate similar signaling pathways, and EMT is essential for metastasis in many tumors [10].

Several studies have shown that the tumor microenvironment (TME) significantly influences tumor progression, promoting tumor migration, drug resistance, and immunosuppression [9,11]. Hypoxia, a lack of oxygen, is a common characteristic of solid tumors, especially in the core regions furthest from blood vessels [11]. Under hypoxic conditions, Tumor cells stabilize HIF-1α, a key transcription factor. HIF-1α binds to specific DNA sequences in target genes, regulating their expression and impacting the tumor microenvironment (TME). Several studies have revealed its multifaceted role. Wang et al. demonstrated that Mindin, an extracellular matrix protein, suppresses HIF-1α expression, thereby inhibiting colon cancer progression [13]. Samanta et al. showed that chemotherapy can induce immune evasion in breast cancer through HIF-1α-mediated upregulation of CD47, CD73, and PDL1 in cancer cells [14]. tumor cells stabilize HIF-1α, a key transcription factor. HIF-1α binds to specific DNA sequences in target genes, regulating their expression and impacting the TME. The impact of low, physiological levels of HIF-1α on lung metastasis in breast cancer remains under investigation, particularly regarding its role in EMT-driven metastasis [12].

Herein, in this study, we aimed to address this gap by knocking down HIF-1α expression in 4T1 breast cancer cells using lentiviral transfection. We then evaluated the effects of HIF-1α knockdown on metastasis in vitro using wound-healing and Transwell assays, and further assessed its impact on lung metastasis in vivo using a mouse model. This work will provide new evidence for better understand the relationship between HIF-1α and breast cancer metastasis, and give more proof for HIF-1a targeted breast cancer therapy.

2. Materials and methods

2.1. Cell culture and lentiviral transfection

4T1 mouse breast cancer cells were purchased from the National Collection of Authenticated Cell Cultures, and maintained in RPMI-1640 (Gibco; Thermo Fisher Scientific, Inc.) supplemented with 10 % FBS (Gibco; Thermo Fisher Scientific, Inc.) and 100U/ml penicillin, 0.1 mg/ml streptomycin (Beijing Solarbio Science & Technology Co., Ltd.). For knockdown of HIF-1A, pHBLV-U6-MCS-shRNA-HIF-1A-GFP-PURO (Hanbio Biotechnology Co., Ltd.) or control shRNA-lentivirus (Hanbio Biotechnology Co., Ltd.) were transfected into 4T1 cells when then reached a density of 40 %, using an MOI (multiplicity of infection) of 20. After 48 h, shRNA-expressing cells were selected by adding 5 μg/ml puromycin to the media for 15 days. The transfection ratio was confirmed by fluorescence microscopy or flow cytometry, and the expression of HIF-1α in 4T1 cells was detected by western blotting and reverse transcription-quantitative (RT-q) PCR.

2.2. Flow cytometry

The transfected 4T1 cells were digested with trypsin and then washed with PBS. Cell suspensions containing 1×10^6 single cells were assessed by flow cytometry using a BD FACS Calibur flow cytometer.

2.3. RT-qPCR

Following treatment, cells were washed with PBS 3 times, and total RNA was extracted using TRIzol reagent. The concentration and purity of the extracted RNA were determined using a NanoDrop spectrophotometer. cDNA was synthesized by RT, according the manufacturer' protocol. The total reaction volume for qPCR was 20 μl, including template cDNA (1 μL), primer mix (2 μl), 2 × SYBR-green mix (10 μl), and RNase-free water up to a final volume of 20 μl. The reaction conditions were based on the manufacturer's instructions. The sequences of the primers were: HIF-1α forward, 5′-TCAGCATACAGTGGCACTCA-3′, and reverse, 5′- AAGGGAGC-CATCATGTTCCA-3'; MMP-2 forward, 5′- ACAAGTGGTCCGCGTAAAGT-3′, and reverse, 5′- AAACAAGGCTTCATGGGGGC-3'; MMP-9 forward, 5′-TGTGTGCTATGTGCACCCTC-3′, and reverse, 5′- TTGGCTTTGGAGGACGACAG-3'; E-cadherin forward, 5′- GACTTAGA-GATTGGCGAATAC-3′, and reverse, 5′- GAGGATGGCAGGAACTTG -3'; Vimentin forward, 5′-CAGCCTCTATTCCTCATCC-3′, and reverse, 5′- AGTTCTACCTTCTCGTTGG-3'; SNAIL forward, 5′- ATGGAGTGCCTTTGTACCCG-3′, and reverse, 5′- CAGTAAC-CACCCTGCTGAGG -3'; GAPDH forward, 5′-GGTTGTCTCCTGCGACTTCA-3′, and reverse, 5′- TGGTCCAGGGTTTCTTACTCC-3'. The results were represented using the relative quantitative method and calculated using the Delta-Delta CT ($2^{-\Delta\Delta CT}$) method.

2.4. Western-blotting

Cells were lysed in RIPA lysis buffer containing Protease inhibitors for 15 min, and the protein concentration was quantified using a BCA protein Assay kit. For each test, 30 μg of total protein was loaded per lane, and western blotting was performed as described previously [13]. The following antibodies were used: β-actin (1:1000; ProteinTech Group, Inc.), HIF-1α (1:1000; Cell Signaling Technology, Inc.), MMP2 (1:1000; ProteinTech Group, Inc.), MMP9 (1:1000; ProteinTech Group, Inc), SNAIL (1:1000; ProteinTech Group, Inc.),E-cadherin (1:1000; ProteinTech Group, Inc), vimentin (1:1000; ProteinTech Group, Inc.), horseradish peroxidase-conjugated anti-rabbit IgG(H&L) (1:1000; ProteinTech Group, Inc.) and horseradish peroxidase-conjugated anti-mouse IgG (H&L) (1:1000; ProteinTech Group, Inc.). Electron chemiluminescence reagent (Milliporpe Sigma) was used to visualize blots, β-actin was used as the loading control and densitometry analysis was performed using ImageJ (National Institutes of Health).

2.5. Wound-healing assay

For wound-healing assays, 100,000 cells were seeded in six-well plates and allowed to adhere overnight. The following day, a clean, straight wound was created using a sterile pipette tip across the cell monolayer. The plate was then washed with PBS to remove detached cells and debris. Fresh media was added, and the wound was monitored and imaged at designated time points, 24, 48, and 72 h. Wound closure was quantified by measuring the scratch width at each time point using a vernier caliper or image analysis software. The wound closure rate was calculated as following: [(initial scratch width - scratch width at time point)/initial scratch width] x 100 %.

2.6. Transwell migration assay

A transwell migration assay was performed to assess cell migration using chambers with 8 μm pores. 3×10^5 cells in 150 μL medium were seeded in the upper chamber of each transwell. The lower chamber contained 500 μL of medium supplemented with 20 % FBS to serve as a chemoattractant. After 24 h of incubation, the transwell inserts were removed, washed, fixed in 4 % formaldehyde for 30 min, stained with 0.25 % crystal violet for 30 min, and imaged. Four fields were randomly selected from each image, and the number of migrated cells in each field was counted. The results are presented as the average number of migrated cells per field.

2.7. Mouse lung metastasis model

All animal experiments were approved by the Ethics Committee of The First Affiliated Hospital of Xinxiang Medical University in accordance with institutional guidelines. Female BABL/C mice (6–8 weeks old) were injected intravenously (tail vein) with 1×10^6 4T1-NC or 4T1-HIF-1α-KD cells. To minimize animal suffering, euthanasia was performed using a CO_2 chamber with a gradual increase in CO_2 concentration (10–30 % per minute) for a total exposure time of 5 min on days 3, 5, 7, 9, 11, and 13. Lungs were then collected for imaging and Hematoxylin and Eosin (H&E) staining. Each group consisted of 6 mice, and the experiment was repeated three times.

2.8. H&E staining and immunohistochemistry

Lung tissues were washed with PBS and fixed overnight in 4 % paraformaldehyde. Following fixation, tissues were paraffin-embedded, and 4 μm sections were prepared for histological analysis. H&E staining was performed according to the manufacture's instructions to assess overall tissue morphology. To evaluate the expression of E-cadherin and Vimentin in the lung, deparaffinization and antigen retrieval were performed on the sections. Endogenous peroxidase activity was quenched with 3 % hydrogen peroxide. After identifying and delineating areas of interest, the sections were blocked with serum to minimize non-specific antibody binding. Subsequently, primary antibodies against E-cadherin (1:100 dilution) and Vimentin (1:100 dilution) were incubated with the tissue sections overnight at 4 °C. After washing, the sections were incubated with the corresponding horseradish peroxidase (HRP)-conjugated secondary antibody at room temperature. Color development was achieved using a 3,3′-diaminobenzidine (DAB) chromogenic substrate kit. Finally, the sections were counterstained with hematoxylin and imaged.

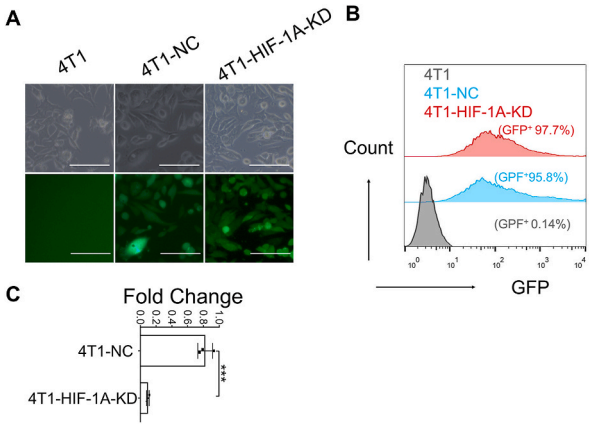

Fig. 1. Knockdown of HIF-1α in 4T1 cells. A) **GFP expression.** Fluorescence microscopy analysis of GFP expression in 4T1-NC (control) and 4T1-HIF-1α-KD (knockdown) cells (scale bars, 100 μm). B) **GFP + cell quantification.** Flow cytometry analysis of the percentage of GFP-positive cells in 4T1, 4T1-NC, and 4T1-HIF-1α-KD groups. C) **HIF-1α mRNA expression.** Quantitative PCR (qPCR) analysis of HIF-1α mRNA levels in 4T1-NC and 4T1-HIF-1α-KD cells relative to the 4T1-NC group (normalized to GAPDH). Data are represented as mean ± standard deviation (SD) from three independent experiments performed in triplicate. Statistical significance was determined using an unpaired *t*-test (***$p < 0.001$ compared to 4T1-NC).

2.9. Statistical analysis

Data were analyzed using GraphPad Prism and unpaired Student's t-tests. Statistical significance was set at $P < 0.05$.

3. Results

3.1. HIF-1α knock-down

4T1 cells were transfected with lentiviral vectors to achieve knockdown of HIF-1α expression. Two lentiviral constructs were used. One is pHBLV-U6-MCS-shRNA-HIF-1A-GFP-PURO, which encoded a short hairpin RNA (shRNA) targeting HIF-1α mRNA for degradation, along with a green fluorescent protein (GFP) reporter gene and a puromycin resistance cassette for selection; the other one is a control, which lacked the shRNA sequence but contained GFP and puromycin resistance for comparison. Following transfection for 15 days, puromycin selection was applied to enrich for stably transfected cells. The resulting cell lines were designated 4T1-HIF-1α-KD (knockdown) and 4T1-NC (control). Fluorescence microscopy confirmed successful transfection, with nearly all cells in both groups exhibiting green fluorescence due to the GFP reporter (Fig. 1A). The Transfection ratio was assessed using a flow cytometer, revealing that over 95 % of the cells expressed GFP (Fig. 1B), indicating successful lentiviral vector delivery. To confirm HIF-1α knockdown, RT-qPCR analysis demonstrated significantly lower HIF-1α mRNA levels in 4T1-HIF-1α-KD cells compared to 4T1-NC cells (Fig. 1C). These combined results confirm the successful transfection of the pHBLV-U6-MCS-shRNA-HIF-1α-GFP-PURO lentivirus and the resulting knockdown of HIF-1α gene expression.

3.2. HIF-1α knockdown inhibited wound healing and migration of 4T1 cells

HIF-1α knockdown was assessed for its impact on various cellular processes in 4T1 cells, including wound healing, migration, proliferation, and apoptosis. While proliferation and apoptosis remained unchanged between control (4T1-NC) and HIF-1α deficient cells (4T1-HIF-1α-KD) (Fig. S1), wound healing was significantly affected (Fig. 2A). Cells with reduced HIF-1α expression displayed slower wound closure compared to control cells at 24, 48, and 72 h. At the earlier 12 h time point, no significant difference in wound healing rate was observed, likely due to insufficient time for migration processes (Fig. S2). Quantification of wound closure rate confirmed a significantly lower rate in 4T1-HIF-1α-KD cells compared to 4T1-NC cells at all later time points (Fig. 2B). Consistent with the wound healing assay, the transwell migration assay using crystal violet staining demonstrated a significantly lower migration rate

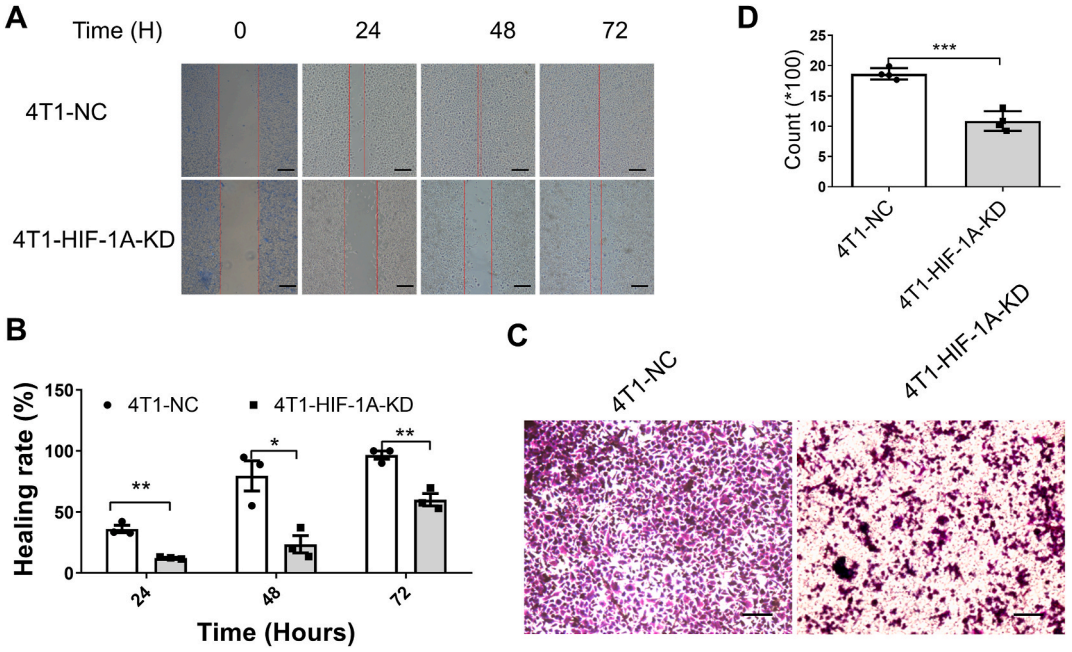

Fig. 2. Low HIF-1α expression reduces 4T1 cell migration and invasion. A) **Wound healing assay.** 4T1-NC and 4T1-HIF-1A-KD cells were wounded with a scratch, and wound closure was monitored after 24, 48, and 72 h (scale bars, 200 μm). B) **Quantification of wound healing assay.** Wound healing rate was calculated from data in panel A. Data are represented as mean ± SD from three independent experiments plated in triplicate. (*$p < 0.05$, **$p < 0.01$, ***$p < 0.001$ compared to 4T1-NC at the same time point). C) **Transwell migration assay.** Migration of 4T1-NC and 4T1-HIF-1A-KD cells through a Matrigel-coated membrane was measured. (scale bars, 100 μm) D) **Quantification of transwell migration assay.** The number of migrated cells was quantified from data in panel C. Data are represented as mean ± SD from three independent experiments plated in triplicate. Statistical significance was determined using an unpaired *t*-test (ns = not significant, *$p < 0.05$, **$p < 0.01$, ***$p < 0.005$ compared to 4T1-NC).

for 4T1-HIF-1α-KD cells compared to control cells (Fig. 2C and D). These findings collectively demonstrate that HIF-1α plays a critical role in promoting both wound healing and migration of 4T1 cells.

3.3. HIF-1α knock down inhibits EMT in 4T1 cells

Since degradation of the extracellular matrix and basement membrane is crucial for cancer cell metastasis, we investigated the expression of MMP-2 and MMP-9, key enzymes involved in this process, in 4T1-NC and 4T1-HIF-1α-KD cells. Both RT-qPCR and western blotting analyses revealed that knockdown of HIF-1α significantly decreased the expression of both MMP-2 and MMP-9 at both the mRNA and protein levels (Fig. 3). To explore the effect of HIF-1α knockdown on the EMT of 4T1 cells, the expression levels of key EMT markers were assessed using RT-qPCR (Fig. 4A). As shown in Fig. 4A, compared to control cells (4T1-NC), HIF-1α knockdown (4T1-HIF-1α-KD) resulted in upregulation of E-cadherin and downregulation of Vimentin and SNAIL. Western blotting confirmed these findings at the protein level (Fig. 4B and C). Full uncropped western blots are presented in Fig. S4 for reference. Collectively, these results suggest that HIF-1α knockdown suppresses EMT in 4T1 breast cancer cells.

3.4. HIF-1α knockdown reduces lung metastasis of 4T1 tumor cells in vivo

To investigate the migratory ability of 4T1 cells in vivo, lung tissues from BABL/C mice were collected at various time points after tail vein injection of 4T1-NC or 4T1-HIF-1A-KD cells. On day 3 post-injection, a small nodule was observed in the 4T1-NC group. Over time, the size and number of nodules increased. However, the 4T1-HIF-1A-KD group exhibited delayed and reduced lung metastasis. In contrast, the 4T1-HIF-1α-KD group exhibited delayed and reduced lung metastasis. The first nodule was observed on day 11, and it was smaller than those seen in the 4T1-NC group (Fig. 5A and B). Additionally, the number of nodules was significantly lower in the 4T1-HIF-1α-KD group compared to the 4T1-NC group (Fig. 5B). These findings suggest that HIF-1α knockdown suppressed lung metastasis of 4T1 cells in mice.

3.5. Expression of EMT markers is decreased in 4T1-HIF-1α-KD formed metastatic nodules in mice

To investigate the contribution of EMT in lung metastasis, immunohistochemical staining was performed on metastatic lung tissue to assess E-cadherin and Vimentin expression. Since lung metastases were first detected on day 9 in the 4T1-HIF-1α-KD group, tissues were collected on days 9, 11, and 13. As shown in Fig. 6A, E-cadherin expression was significantly higher in the 4T1-HIF-1α-KD group compared to the 4T1-NC group. Conversely, Vimentin expression was significantly lower in the 4T1-HIF-1α-KD group compared to the 4T1-NC group (Fig. 6B). These results showed that HIF-1α knockdown may suppress lung metastasis by inhibiting EMT in breast cancer cells.

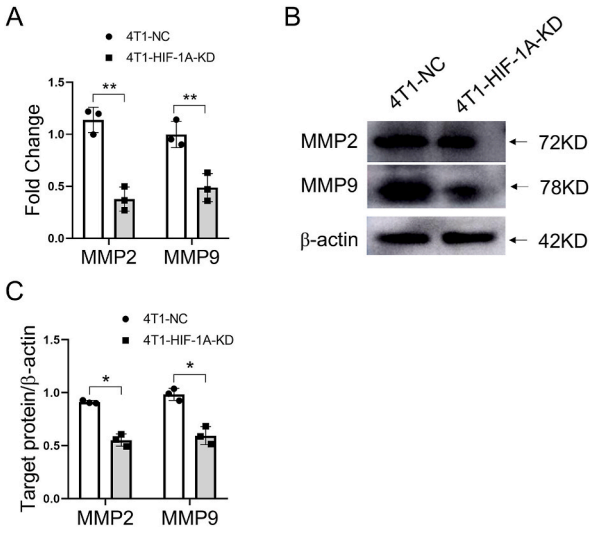

Fig. 3. HIF-1α knockdown reduces MMP-2 and MMP-9 expression in 4T1 cells. A)**MMP-2 and MMP-9 mRNA expression.** qRT-PCR analysis of MMP-2 and MMP-9 mRNA levels in 4T1-HIF-1α-KD cells relative to 4T1-NC cells (normalized to β-actin). Data are represented as mean ± SD from three independent experiments performed in triplicate. Statistical significance was determined using the Delta-Delta CT method. B) **MMP-2 and MMP-9 protein expression.** Western blot analysis of MMP-2 and MMP-9 protein levels in 4T1-NC and 4T1-HIF-1α-KD cells. β-actin served as a loading control. C) **Quantification of Western blot.** Band intensities were quantified using ImageJ software. Data are represented as the ratio of target protein to β-actin and shown as mean ± SD from three independent experiments performed in triplicate. Statistical significance was determined using unpaired t-tests (ns = not significant, *$p < 0.05$, **$p < 0.01$ compared to 4T1-NC).

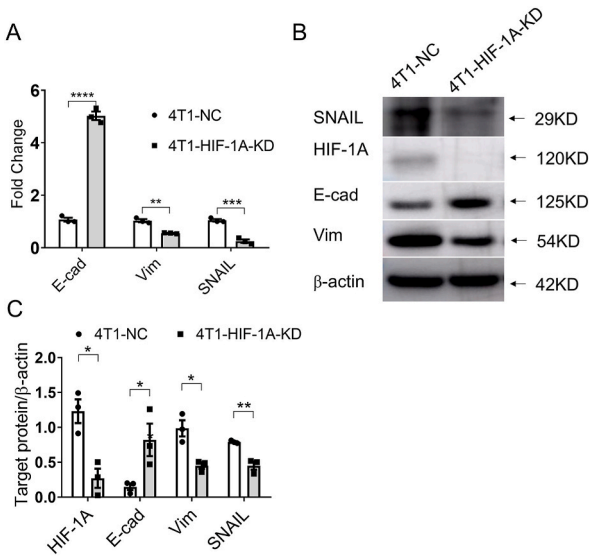

Fig. 4. HIF-1A knockdown regulates EMT markers in 4T1 cells. A) **mRNA expression of EMT markers.** qRT-PCR analysis of SNAIL, E-cadherin, and Vimentin mRNA levels in 4T1-HIF-1α-KD cells relative to 4T1-NC cells (normalized to GAPDH). Data are represented as mean ± SD from three independent experiments performed in triplicate. Statistical significance was determined using the ΔΔCt method. (*$p < 0.05$ compared to 4T1-NC). B) **Protein expression of HIF-1α and EMT markers.** Western blot analysis of HIF-1α, SNAIL, E-cadherin, and Vimentin protein levels in 4T1-NC and 4T1-HIF-1α-KD cells. β-actin served as a loading control (Full uncropped western blots are shown in Supplementary Fig. 3.). C) **Quantification of Western blot.** Band intensities were quantified using ImageJ software. Data are represented as the ratio of target protein to β-actin and shown as mean ± SD from three independent experiments performed in triplicate. Statistical significance was determined using unpaired t-tests (ns = not significant, *$p < 0.05$, **$p < 0.01$, ***$p < 0.005$, ****$p < 0.001$ compared to 4T1-NC).

4. Discussion

HIF-1α, a transcription factor, plays a critical role in tumor survival [14]. Tumors often experience hypoxia, and under these conditions, HIF-1α degradation is inhibited [15], allowing it to accumulate and translocate to the nucleus. There, HIF-1α binds to hypoxia response elements (HRE) in the DNA of target genes [16]. This binding activates the transcription of over 200 genes, collectively enabling tumor cells to survive and adapt to the hypoxic environment [17]. In the present study, it was demonstrated that knocking down HIF-1α expression under normal conditions reduces breast cancer cell metastasis in both cell culture and animal models. HIF-1α knockdown decreases the expression of MMP-2 and MMP-9, proteins that degrade the extracellular matrix and basement membrane, crucial for cell migration [18,19]. Additionally, the expression of Vimentin, a protein that promotes migration, was down-regulated, while the expression of E-cadherin, the adhesion protein, was up-regulated at both the mRNA and protein levels (Fig. 3).As a cellular adhesion molecule, E-cadherin plays a critical role in epithelial cancers by regulating cell-to-cell adhesion and inhibiting cell growth [20]. It is generally considered a metastasis suppressor protein, and its loss is associated with increased tumor aggressiveness, as observed in this study. However, some studies suggest E-cadherin can promote metastasis in specific environments. Understanding this dual role is essential for a more complete picture of how E-cadherin influences tumor metastasis. Understanding its dual roles is essential for a more complete picture of how E-cadherin influences tumor metastasis. Similar to findings in ovarian carcinoma and VHL-deficient renal cell carcinoma [21,22], this study demonstrated that HIF-1α regulates E-cadherin expression in mouse breast cancer cells.

Vimentin, a key regulator of various cellular processes like migration, differentiation, and adhesion, was downregulated following HIF-1α knockdown in this study [23–25]. This suggests a potential role for HIF-1α in regulating metastasis through Vimentin. However, it's important to acknowledge that EMT is a complex multistep process. While markers like SNAIL, E-cadherin, and Vimentin provide valuable insights, analyzing only a limited panel presents an incomplete picture. This represents a limitation of the current study.

Of note, in the mouse metastasis model, normal 4T1 cells migrated to the lungs by day 3, while HIF-1α knockdown 4T1 cells were not observed until day 11. Lung metastasis was assessed by counting nodules and using H&E staining. However, incorporating imaging techniques, such as bioluminescent imaging with IVIS, would strengthen the results by providing real-time monitoring of tumor development.

This study demonstrates that HIF-1α, a transcription factor in breast cancer cells, promotes metastasis. Reducing HIF-1α expression may be a promising strategy to inhibit breast cancer spread.

In conclusion, knocking down HIF-1α suppressed breast cancer metastasis, highlighting its critical role in EMT and metastasis. These findings strengthen the rationale for targeting HIF-1α as a therapeutic approach for breast cancer.

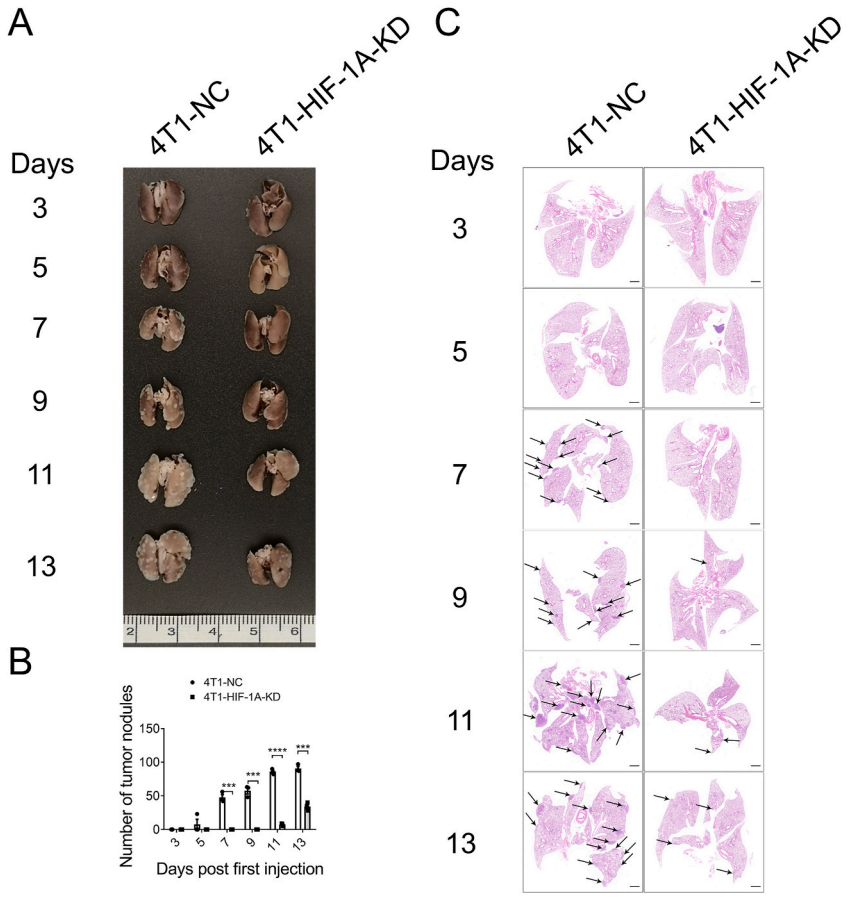

Fig. 5. HIF-1α knockdown suppresses lung metastasis of 4T1 cells in mice. A) **Lung metastasis nodules.** Representative images of lung nodules (arrows) in mice inoculated with 4T1-NC (control) or 4T1-HIF-1A-KD (knockdown) cells at different time points. (n = 3 mice per group). B) **Quantification of lung metastasis nodules.** Number of lung metastasis nodules in mice inoculated with 4T1-NC or 4T1-HIF-1A-KD cells. Data are represented as mean ± SD from three independent experiments. Statistical significance was determined using an unpaired *t*-test (ns = not significant, ***p < 0.005, ****p < 0.001 compared to 4T1-NC). C) **H&E staining of lung tissues.** Representative images of H&E-stained lung sections from mice inoculated with 4T1-NC or 4T1-HIF-1α-KD cells (scale bars, 1000 μm).

Ethics statement

This study was conducted according to Ethics Committee of The First Affiliated Hospital of Xinxiang Medical University (2020047). All research has been performed in accordance with the Declaration of Helsinki. All mouse experimental protocols were approved by the Ethics Committee of The First Affiliated Hospital of Xinxiang Medical University. All tests were carried out by the Ethics Committee of The First Affiliated Hospital of Xinxiang Medical University. We confirm that all methods are reported in accordance with ARRIV guidelines for the reporting of animal experiments.

Consent for publication

Not applicable.

Data availability statement

The data associated with this study have not deposit into a publicly available. The date in this study will be made available on reasonable request.

The authors declare no conflicts of interest.

CRediT authorship contribution statement

Jinjin Zhao: Writing – review & editing, Writing – original draft, Formal analysis, Data curation. **Haiguang Zhang:** Project

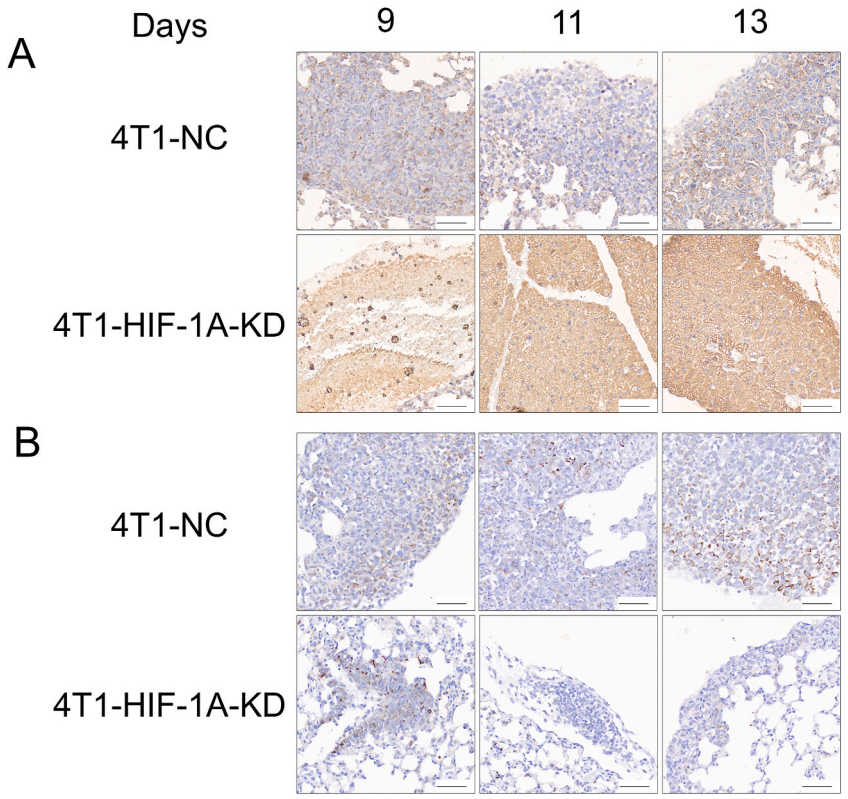

Fig. 6. EMT participated in lung metastasis of mouse breast cancer. A) **E-cadherin expression.** Immunohistochemical staining for E-cadherin (epithelial marker) in lung metastasis tissues from mice with breast cancer. Scale bar, 50 μm B) **Vimentin expression.** Immunohistochemical staining for Vimentin (mesenchymal marker) in lung metastasis tissues from mice with breast cancer. Scale bar, 50 μm.

administration. **Yaqian Liu:** Project administration. **Guangjian Lu:** Resources. **Zhaohui Wang:** Resources. **Qingjiang Mo:** Resources. **Guoqiang Wang:** Resources. **Yanfei Shen:** Writing – review & editing, Writing – original draft, Funding acquisition. **Luyang Jiao:** Funding acquisition, Data curation, Conceptualization.

Declaration of competing interest

The authors declare no conflicts of interest.

Acknowledgements

This study was supported by the National Natural Science Foundation of China (grant number 22074015).

Appendix A. Supplementary data

Supplementary data to this article can be found online at https://doi.org/10.1016/j.heliyon.2024.e37900.

References

[1] Y. Sun, Z. Wang, L. Na, D. Dong, W. Wang, C. Zhao, FZD5 contributes to TNBC proliferation, DNA damage repair and stemness, Cell Death Dis. 11 (12) (2020), https://doi.org/10.1038/s41419-020-03282-3.
[2] C.E. DeSantis, J. Ma, M.M. Gaudet, L.A. Newman, K.D. Miller, A. Goding Sauer, et al., Breast cancer statistics, 2019, Ca - Cancer J. Clin. 69 (6) (2019) 438–451, https://doi.org/10.3322/caac.21583.
[3] X. Shi, Y. Cheng, J. Wang, H. Chen, X. Wang, X. Li, et al., 3D printed intelligent scaffold prevents recurrence and distal metastasis of breast cancer, Theranostics 10 (23) (2020) 10652–10664, https://doi.org/10.7150/thno.47933.
[4] S. Donzelli, E. Milano, M. Pruszko, A. Sacconi, S. Masciarelli, I. Iosue, et al., Expression of ID4 protein in breast cancer cells induces reprogramming of tumour-associated macrophages, Breast Cancer Res. 20 (1) (2018), https://doi.org/10.1186/s13058-018-0990-2. PubMed PMID: WOS:000435887500002.

[5] T. McFall, B. McKnight, R. Rosati, S. Kim, Y. Huang, N. Viola-Villegas, et al., Progesterone receptor A promotes invasiveness and metastasis of luminal breast cancer by suppressing regulation of critical microRNAs by estrogen, J. Biol. Chem. 293 (4) (2018) 1163–1177, https://doi.org/10.1074/jbc.M117.812438.
[6] C. Li, Q. Wang, S. Shen, X. Wei, G. Li, Oridonin inhibits VEGF-A-associated angiogenesis and epithelial-mesenchymal transition of breast cancer in vitro and in vivo, Oncol. Lett. 16 (2) (2018) 2289–2298, https://doi.org/10.3892/ol.2018.8943. PubMed PMID: 30008931.
[7] X. Ye, T. Brabletz, Y. Kang, G.D. Longmore, M.A. Nieto, B.Z. Stanger, et al., Upholding a role for EMT in breast cancer metastasis, Nature 547 (7661) (2017) E1–E3, https://doi.org/10.1038/nature22816. PubMed PMID: 28682326.
[8] L. Yang, N. Li, Z. Xue, L. Liu, J. Li, X. Huang, et al., Synergistic therapeutic effect of combined PDGFR and SGK1 inhibition in metastasis-initiating cells of breast cancer, Cell Death Differ. 27 (7) (2020) 2066–2080, https://doi.org/10.1038/s41418-019-0485-4.
[9] Y. Chen, B. Zhang, L. Bao, L. Jin, M. Yang, Y. Peng, et al., ZMYND8 acetylation mediates HIF-dependent breast cancer progression and metastasis, J. Clin. Invest. 128 (5) (2018) 1937–1955, https://doi.org/10.1172/JCI95089.
[10] G. Lin, J. Li, J. Cai, H. Zhang, Q. Xin, N. Wang, et al., RNA-Binding protein MBNL2 regulates cancer cell metastasis through MiR-182-MBNL2-AKT pathway, J. Cancer 12 (22) (2021) 6715–6726, https://doi.org/10.7150/jca.62816.
[11] F. Zheng, J. Chen, X. Zhang, Z. Wang, J. Chen, X. Lin, et al., The HIF-1α antisense long non-coding RNA drives a positive feedback loop of HIF-1α mediated transactivation and glycolysis, Nat. Commun. 12 (1) (2021), https://doi.org/10.1038/s41467-021-21535-3.
[12] L. Xiang, G.L. Semenza, Hypoxia-inducible factors promote breast cancer stem cell specification and maintenance in response to hypoxia or cytotoxic chemotherapy, Adv. Cancer Res. 141 (2019) 175–212, https://doi.org/10.1016/bs.acr.2018.11.001. PubMed PMID: 30691683.
[13] J. Zhao, N. Pan, F. Huang, M. Aldarouish, Z. Wen, R. Gao, et al., Vx3-Functionalized alumina nanoparticles assisted enrichment of ubiquitinated proteins from cancer cells for enhanced cancer immunotherapy, Bioconjugate Chem. 29 (3) (2018) 786–794, https://doi.org/10.1021/acs.bioconjchem.7b00578. PubMed PMID: 29382195.
[14] F. Hajizadeh, I. Okoye, M. Esmaily, M. Ghasemi Chaleshtari, A. Masjedi, G. Azizi, et al., Hypoxia inducible factors in the tumor microenvironment as therapeutic targets of cancer stem cells, Life Sci. 237 (2019) 116952, https://doi.org/10.1016/j.lfs.2019.116952.
[15] X. Cao, W. Wu, D. Wang, W. Sun, S. Lai, Glycogen synthase kinase GSK3α promotes tumorigenesis by activating HIF1/VEGFA signaling pathway in NSCLC tumor, Cell Commun. Signal. 20 (1) (2022) 32, https://doi.org/10.1186/s12964-022-00825-3. PubMed PMID: 35292059.
[16] E.B. Rankin, A.J. Giaccia, The role of hypoxia-inducible factors in tumorigenesis, Cell Death Differ. 15 (4) (2008) 678–685, https://doi.org/10.1038/cdd.2008.21.
[17] J. Qian, E.B. Rankin, Hypoxia-induced phenotypes that mediate tumor heterogeneity, Adv. Exp. Med. Biol. 1136 (2019) 43–55, https://doi.org/10.1007/978-3-030-12734-3_3. PubMed PMID: 31201715.
[18] Q. Li, J. Li, K. Wang, L. Liao, Y. Li, H. Liang, et al., Activation of sphingomyelin phosphodiesterase 3 in liver regeneration impedes the progression of colorectal cancer liver metastasis via exosome-bound intercellular transfer of ceramides, Cell Mol Gastroenter 16 (3) (2023) 385–410, https://doi.org/10.1016/j.jcmgh.2023.05.007.
[19] K. Wadowska, P. Błasiak, A. Rzechonek, M. Śliwińska-Mossoń, Analysis of MMP-2-735C/T (rs2285053) and MMP-9-1562C/T (rs3918242) polymorphisms in the risk assessment of developing lung cancer, Int. J. Mol. Sci. 24 (13) (2023) 10576, https://doi.org/10.3390/ijms241310576.
[20] D. Hanahan, R.A. Weinberg, The hallmarks of cancer, Cell 100 (1) (2000) 57–70, https://doi.org/10.1016/S0092-8674(00)81683-9.
[21] T. Imai, A. Horiuchi, C. Wang, K. Oka, S. Ohira, T. Nikaido, et al., Hypoxia attenuates the expression of E-cadherin via up-regulation of SNAIL in ovarian carcinoma cells, Am. J. Pathol. 163 (4) (2003) 1437–1447, https://doi.org/10.1016/S0002-9440(10)63501-8.
[22] M.A. Esteban, M.G.B. Tran, S.K. Harten, P. Hill, M.C. Castellanos, A. Chandra, et al., Regulation of E-cadherin expression by VHL and hypoxia-inducible factor, Cancer Res. 66 (7) (2006) 3567–3575.
[23] Z. Chen, Z. Fang, J. Ma, Regulatory mechanisms and clinical significance of vimentin in breast cancer, Biomed. Pharmacother. 133 (2021) 111068, https://doi.org/10.1016/j.biopha.2020.111068.
[24] F. Cheng, Y. Shen, P. Mohanasundaram, M. Lindström, J. Ivaska, T. Ny, et al., Vimentin coordinates fibroblast proliferation and keratinocyte differentiation in wound healing via TGF-β–Slug signaling, Proc. Natl. Acad. Sci. USA 113 (30) (2016), https://doi.org/10.1073/pnas.1519197113.
[25] S. Wen, Y. Hou, L. Fu, L. Xi, D. Yang, M. Zhao, et al., Cancer-associated fibroblast (CAF)-derived IL32 promotes breast cancer cell invasion and metastasis via integrin β3–p38 MAPK signalling, Cancer Lett. 442 (2019) 320–332, https://doi.org/10.1016/j.canlet.2018.10.015.